Electronic Supplementary Information

D-π*-A type planar chiral thermally activated delayed fluorescence materials for efficient circularly polarized electroluminescence

Da-Wei Zhang,[a,b,#] Jing-Min Teng,[a,b,#] Yin-Feng Wang,[a,b] Xiao-Ni Han,[a,b] Meng Li[a,*] and Chuan-Feng Chen[a,b,*]

[a]*Beijing National Laboratory for Molecular Sciences, CAS Key Laboratory of Molecular Recognition and Function, Institute of Chemistry, Chinese Academy of Sciences, Beijing 100190, China.*

[b]*University of Chinese Academy of Sciences, Beijing 100049, China.*

E-mail: cchen@iccas.ac.cn, limeng@iccas.ac.cn

Contents

1. General information

All the reagents and solvents were purchased from commercial sources and used without further purification. ^{1}H and ^{13}C NMR spectra were recorded on Brucker 300 or 400 MHz NMR spectrometers in $CDCl_3$ solutions. High resolution mass spectra were measured on a Thermo Fisher® Exactive high resolution LC-MS spectrometer. Thermal gravimetric analyses (TGA) were performed on a TA Instruments TGA 2050 thermal analyzer at a heating rate of 20 °C/min in nitrogen. Cyclic voltammetry was performed using a CHI600A analyzer with a scan rate of 100 mV/s at room temperature to investigate the oxidation potentials. Single crystals of emitters suitable for X-ray diffraction analyses were obtained from their solution in toluene/ethanol. Crystal structures were solved with direct methods and refined with a full-matrix least-squares technique, using the SHELXS software package. UV-Vis spectra were recorded on PerkinElmer® Lambda 950 UV-Vis/NIR spectrometer, and the fluorescence spectra were recorded on HITACHI® F-7000 Fluorescence Spectrometer. CD spectra were recorded on automatic mode using BioLogic MOS-450 spectropolarimete, and the CPL and CPEL spectra were measured with a JASCO CPL-300 spectrometer at room temperature. The transient photoluminescence decay characteristics and temperature dependence experiments and absolute PL quantum yield were measured on an Edinburgh Instruments FLS1000 spectrometer. The devices were manufactured through vacuum evaporation machine model OMV-FS450 FANGSHENG.

OLED fabrication. After carefully cleaning, the ITO substrates were rinsed in an ultrasonic bath with anhydrous ethanol and then dried under the temperature of 110 °C before treated by oxygen plasma. Finally, all kinds of materials were evaporated on the glass substrate in turn.

Theoretical Calculations Method. The ground state geometries of gas state were fully optimized by B3LYP method including Grimme's dispersion correction with 6-31G (d) basis set using Gaussian 09 software package.[S1] The HOMO and LUMO were visualized with Gaussview 6.0.

2. Synthesis procedure, NMR spectra, high-resolution mass analyses and single crystal

2.1 Synthesis procedure

Synthesis of 4-bromo-7-(tert-butoxycarbonyl)amino[2.2]paracyclophane (Br-PCP-NHBoc)

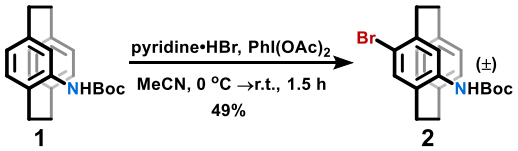

Scheme S1. Synthesis of *rac*-**Br-PCP-NHBoc**.

To a solution of *N*-*tert*-butyl-[2.2]paracyclophane-4-ylcarbamate **1** (3.23 g, 10 mmol, 1.0 equiv) in acetonitrile (100 mL) at 0 °C was added pyridine hydrobromide (1.92 g, 12 mmol, 1.2 equiv) and $PhI(OAc)_2$ (3.87 g, 12 mmol, 1.2 equiv). The reaction mixture was stirred 30 min. at 0 °C and 1 h at room temperature. The solvent was removed under reduced pressure and the product was purified by column chromatography (petroleum ether/ethyl acetate 25:1, v/v) to provide the titled compound as a white solid (1.97g, 4.9mmol, 49%).[S2]

M.p.: 157-160 °C; ^{1}H NMR (500 MHz, $CDCl_3$): δ 7.11 (d, *J* = 7.8 Hz, 1H), 6.78 (s, 1H), 6.77 (s, 1H), 6.50 (d, *J* = 7.7 Hz, 1H), 6.44 (s, 1H), 6.41 (d, *J* = 7.8 Hz, 1H), 6.30 (s, 1H), 3.36 (dd, *J* = 17.1, 6.1 Hz, 1H), 3.19-3.09 (m, 3H), 3.05-2.96 (m, 2H), 2.76-2.70 (m, 1H), 2.64-2.57 (m, 1H), 1.54 (s, 9H); ^{13}C NMR (126 MHz, $CDCl_3$): δ 152.5, 140.1, 139.1, 138.5, 138.4, 136.5, 132.4, 129.6, 129.0, 126.6, 120.8, 80.7, 35.4, 33.4, 33.2, 32.4, 28.3; HR-MS (ESI): m/z calcd for $C_{21}H_{23}O_2NBr^-$ $[M-H]^-$ 400.0918, found 400.0922.

Synthesis of 4-bromo-7-amino[2.2]paracyclophane (Br-PCP-NH_2)

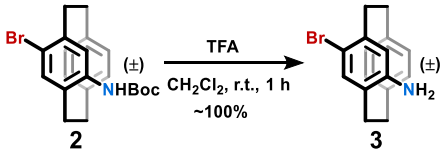

Scheme S2. Synthesis of *rac*-**Br-PCP-NH_2**.

To a solution of *rac*-**Br-PCP-NHBoc 2** (2.01 g, 5 mmol, 1.0 equiv) in anhydrous dichloromethane (30 mL), trifluoroacetic acid (7 mL) was added and stirred for 2 h at room temperature. Then, the excess reagent and solvent were removed under

reduced pressure. The resulting sticky viscous mass was neutralized by saturated NaOH solution (*pay attention to the intense heat release during neutralization*) and extracted with dichloromethane (3 × 30 mL) and then with brine (2 × 20 mL), dried over anhydrous $MgSO_4$, and evaporated under reduced pressure. The crude compound was further used without purification.

^{1}H NMR (400 MHz, $CDCl_3$): δ 7.14 (t, *J* = 6.2 Hz, 2H), 6.41 (dd, *J* = 13.9, 7.8 Hz, 2H), 6.30 (s, 1H), 5.40 (s, 1H), 3.44 (br, 2H), 3.32 (d, *J* = 12.0 Hz, 1H), 3.23–3.12 (m, 1H), 3.11–3.05 (m, 2H), 3.00 (t, *J* = 11.0 Hz, 2H), 2.62–2.49 (m, 2H); ^{13}C NMR (101 MHz, $CDCl_3$): δ 144.5, 139.9, 138.9, 138.7, 138.6, 132.9, 131.7, 129.8, 128.0, 126.3, 123.7, 115.0, 35.5, 33.3, 32.6, 31.9; HR-MS (ESI): *m/z* calcd for $C_{16}H_{15}NBr^-$ $[M-H]^-$ 300.0393, found 300.0396.

Synthesis 4-iodo-7-bromo[2.2]paracyclophane (I-PCP-Br)

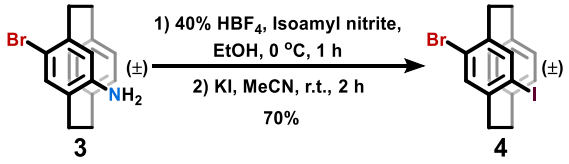

Scheme S3. Synthesis of *rac*-**I-PCP-Br**.

To a solution of *rac*-**Br-PCP-NH$_2$ 3** (1.51 g, 5 mmol, 1.0 equiv) in ethanol (10 mL), 40% HBF_4 acid (2.5 mL, 15 mmol, 3.0 equiv) was added and stirred at 60 °C, until a clear solution was resulted. After 10 min, the solution was cooled at -5 °C, and then isoamyl nitrite (2 mL, 15 mmol, 3.0 equiv) was added dropwise. The temperature was kept at –5 °C and stirring was continued for another 1 h. Diethyl ether (20 mL) was added, and then the resulting precipitate was filtered, washed with diethyl ether (20 mL), and finally dried under vacuum to obtain the diazonium fluoroborate (1.62-1.69 g) which was used without further purification. The diazonium fluoroborate (1.65 g, 4.18 mmol) was added to a mixture of acetonitrile (35 mL) and potassium iodide (1.37 g, 8.25 mmol) at room temperature. After a rapid evolution of nitrogen, the mixture was kept for 2 h at room temperature. The solvent was removed, and the residue was purified by chromatography on silica gel using petroleum ether as eluent to furnish the desired product as a white solid (1.45g, 3.5 mmol, 70%).[S3]

M.p.: 200-203 °C; ^{1}H NMR (400 MHz, $CDCl_3$): δ 7.23 (s, 1H), 7.18 (d, *J* = 7.9 Hz, 1H), 6.77 (s, 1H), 6.47 (d, *J* = 7.8 Hz, 2H), 6.43 (s, 1H), 3.43–3.28 (m, 2H), 3.26–3.15 (m, 2H), 3.07 (dd, *J* = 22.7, 11.3 Hz, 2H), 2.88–2.77 (m, 1H), 2.73-2.65 (m, 1H); ^{13}C NMR (101 MHz, $CDCl_3$): δ 144.8, 144.3, 141.0, 139.0, 138.7, 137.6, 132.6, 132.5, 129.6, 129.2, 126.6, 101.8, 38.9, 35.4, 33.3, 33.2; HR-MS (APCI): *m/z* calcd for $C_{16}H_{15}BrI^+$ $[M+H]^+$ 412.9396, found 412.9393.

Synthesis of 4-bromo-7-(4,6-diphenyl-1,3,5-triazin-2-yl)[2.2]paracyclophane (Br-PT)

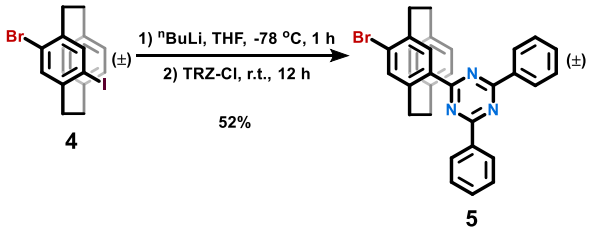

Scheme S4. Synthesis of *rac*-**Br-PT**.

To a solution of *rac*-**I-PCP-Br 4** (2.9 g, 7 mmol, 1.0 equiv) in anhydrous tetrahydrofuran (25 mL) under N_2 atmosphere, *n*-BuLi (4.2 mL, 2.5 M in *n*-hexane) was added dropwise at -78 °C. The mixture was continued stirred for another 1 h. Then, to the solution was added anhydrous tetrahydrofuran (20 mL) dissolved with 2-chloro-4,6-diphenyl-1,3,5-triazine (TRZ-Cl, 1.31 g, 4.9 mmol, 0.7 equiv). The solution was warmed to room temperature and stirred for 12 h. H_2O (1 mL) was added and after 10 min the solvent removed in *vacuo*. The product was purified by column chromatography (petroleum ether/DCM 4:1, v/v) to provide the titled compound as a white solid (1.30 g, 2.51 mmol, 52%).

M.p.: 175-177 °C; ^{1}H NMR (400 MHz, $CDCl_3$): δ 8.76 (d, *J* = 4.8 Hz, 4H), 7.73 (s, 1H), 7.68–7.56 (m, 6H), 7.19 (d, *J* = 7.8 Hz, 1H), 6.71 (s, 1H), 6.57 (d, *J* = 7.8 Hz, 1H), 6.53 (d, *J* = 7.8 Hz, 1H), 6.45 (d, *J* = 7.7 Hz, 1H), 4.67–4.56 (m, 1H), 3.58–3.41 (m, 1H), 3.31–3.13 (m, 3H), 3.08–2.77 (m, 3H); ^{13}C NMR (101 MHz, $CDCl_3$): δ 172.7, 171.7, 143.7, 140.3, 139.6, 139.6, 139.3, 137.4, 136.3, 136.1, 132.7, 132.6, 132.1, 131.5, 130.6, 129.03, 128.98, 128.8, 36.3, 35.8, 35.2, 33.2; HR-MS (ESI): *m/z* calcd for $C_{31}H_{25}N_3Br^+$ $[M+H]^+$ 518.1226, found 518.1213.

Synthesis of 4-(10*H*-phenoxazin-10-yl)-7-(4,6-diphenyl-1,3,5-triazin-2-yl)[2.2]paracyclophane(PXZ-PT)

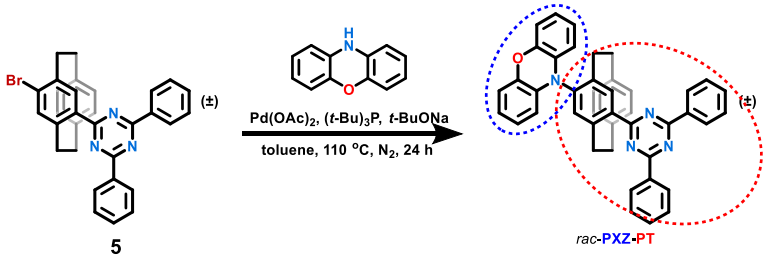

Scheme S5. Synthesis of *rac*-**PXZ-PT**.

Outside a glovebox, *rac*-**Br-PT 5** (1.50 g, 2.89 mmol, 1.0 equiv), 10*H*-phenoxazine (0.79 g, 4.33 mmol, 1.5 equiv), palladium (II) acetate (64.9 mg, 0.29 mmol, 0.1 equiv) and cesium carbonate (2.23g, 11.56 mmol, 4.0 equiv) were added in a Schlenk tube (250 mL). Then, the Schlenk tube was taken into the glovebox and tri-*tert*-butylphosphine (2.2 mL, 0.3 equiv, 10% in toluene) as well as toluene (70 mL) was added. The resulting mixture was taken out of the glovebox and stirred under N_2 atmosphere at 110 °C for 24 h. After cooled to room temperature, the solvent was removed under reduced pressure and the product was purified by column chromatography (petroleum ether/dichloromethane 5:1, v/v) to provide the titled compound as a yellow solid (1.59g, 2.57 mmol, 89%).

M.p.: 270-271 °C; ^{1}H NMR (400 MHz, $CDCl_3$): δ 8.85 (d, *J* = 7.2 Hz, 4H), 8.04 (s, 1H), 7.77-7.62 (m, 6H), 7.18 (s, 1H), 6.90-6.81 (m, 8H), 6.75 (dd, *J* = 12.3, 8.1 Hz, 2H), 6.48 (d, *J* = 7.6 Hz, 1H), 6.35 (d, *J* = 7.8 Hz, 1H), 5.01–4.90 (m, 1H), 3.52–3.31 (m, 2H), 3.26-3.16 (m, 2H), 3.14–3.07 (m, 1H), 3.06–2.95 (m, 2H); ^{13}C NMR (101 MHz, $CDCl_3$): δ 172.1, 171.7, 146.4, 144.3, 139.7, 139.5, 139.4, 136.4, 136.3, 132.7, 132.6, 132.1, 131.8, 131.0, 129.0, 128.9, 123.2, 122.5, 116.3, 115.8, 37.9, 35.1, 34.7, 31.8. HR-MS (ESI): $C_{43}H_{33}ON_4^+[M+H]^+$ 621.2649, found 621.2655; Anal. calcd. (%) for $C_{43}H_{32}N_4O$: C 83.20, H 5.20, N 9.03; found: C 82.96, H 5.14, N 8.86.

2.2 NMR spectra

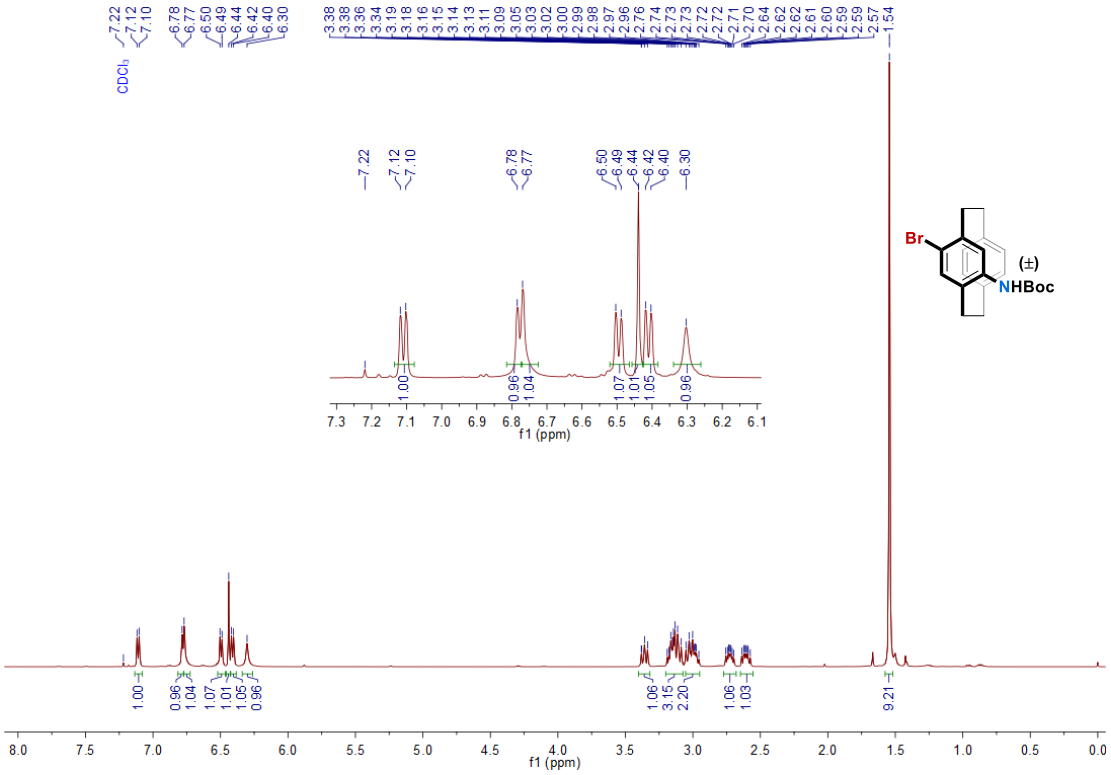

Fig. S1. ^{1}H NMR spectrum of *rac*-**Br-PCP-NBoc**.

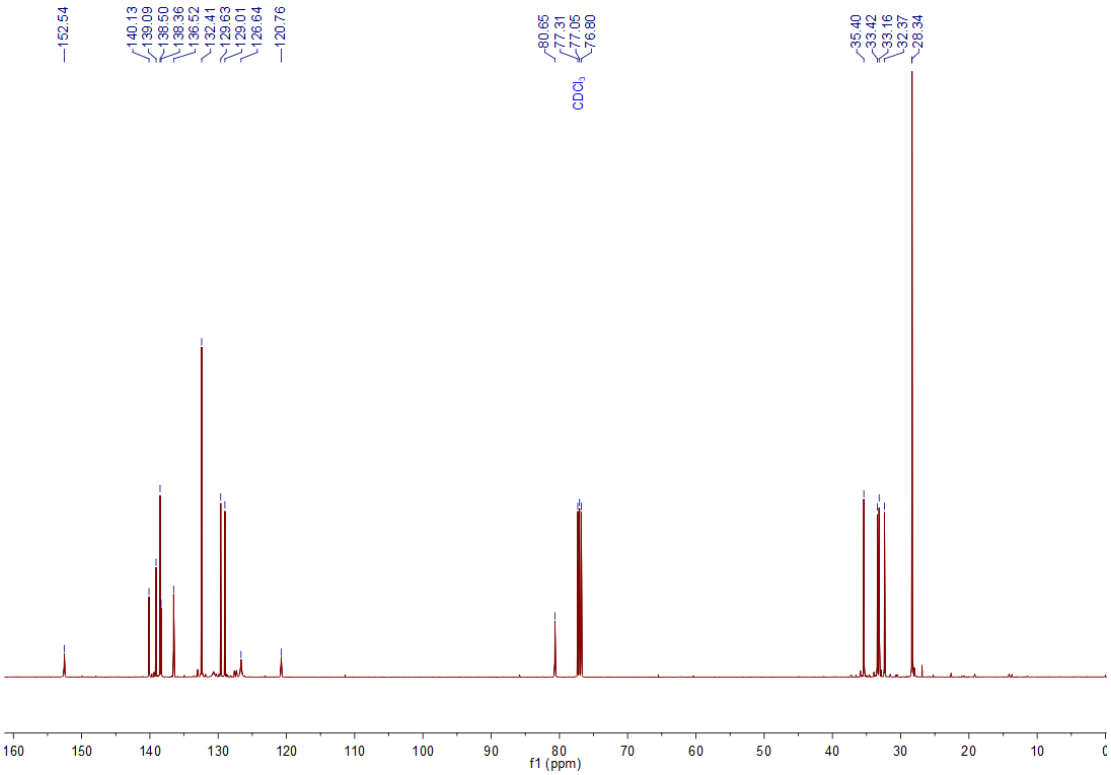

Fig. S2. ^{13}C NMR spectrum of *rac*-**Br-PCP-NBoc**.

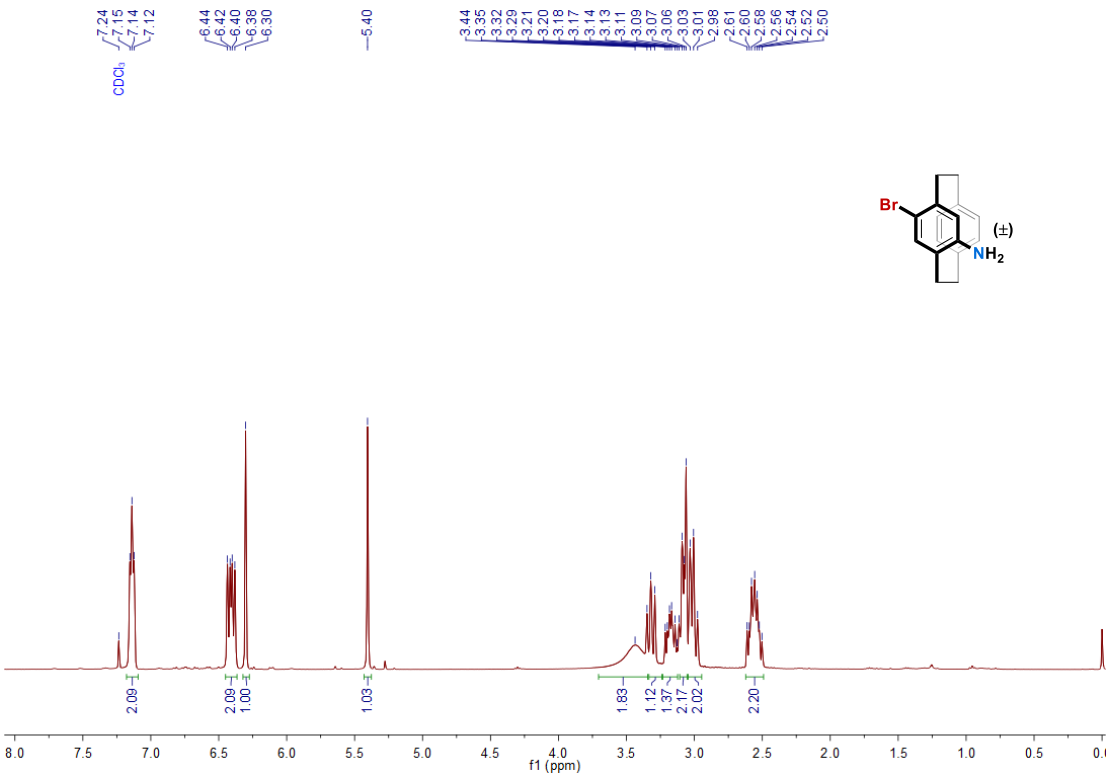

Fig. S3. ^{1}H NMR spectrum of *rac*-**Br-PCP-NH$_2$**.

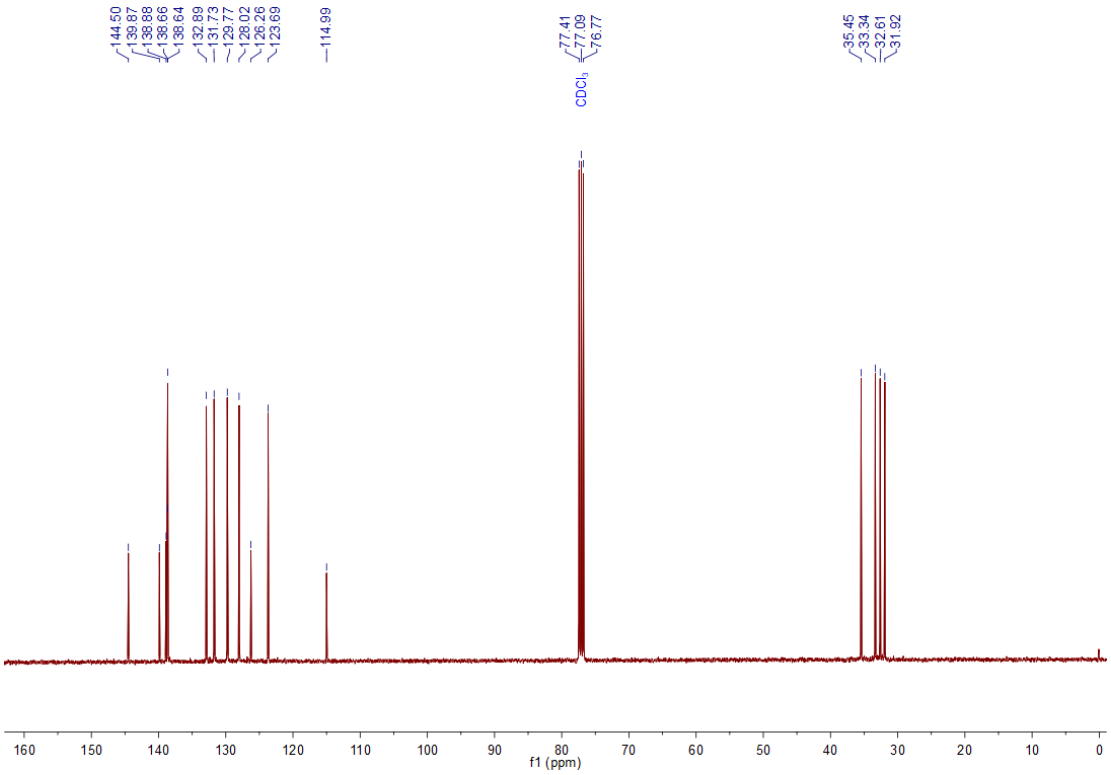

Fig. S4. ^{13}C NMR spectrum of *rac*-**Br-PCP-NH$_2$**.

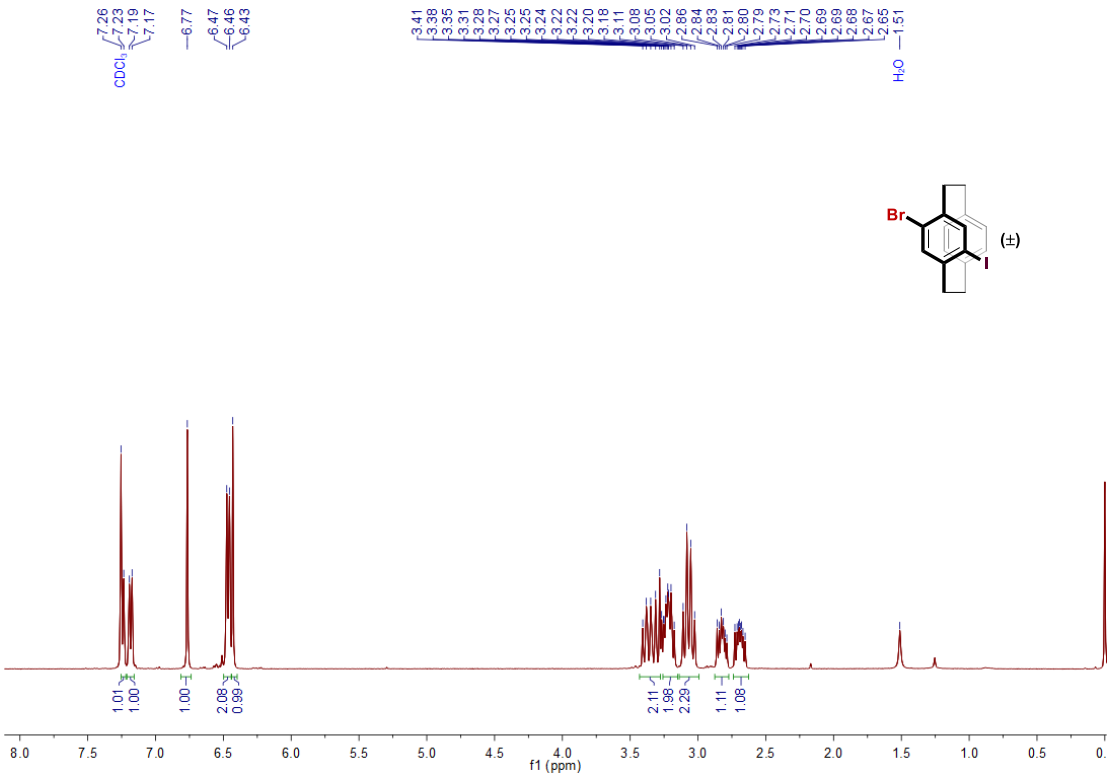

Fig. S5. ^{1}H NMR spectrum of *rac*-**I-PCP-Br**.

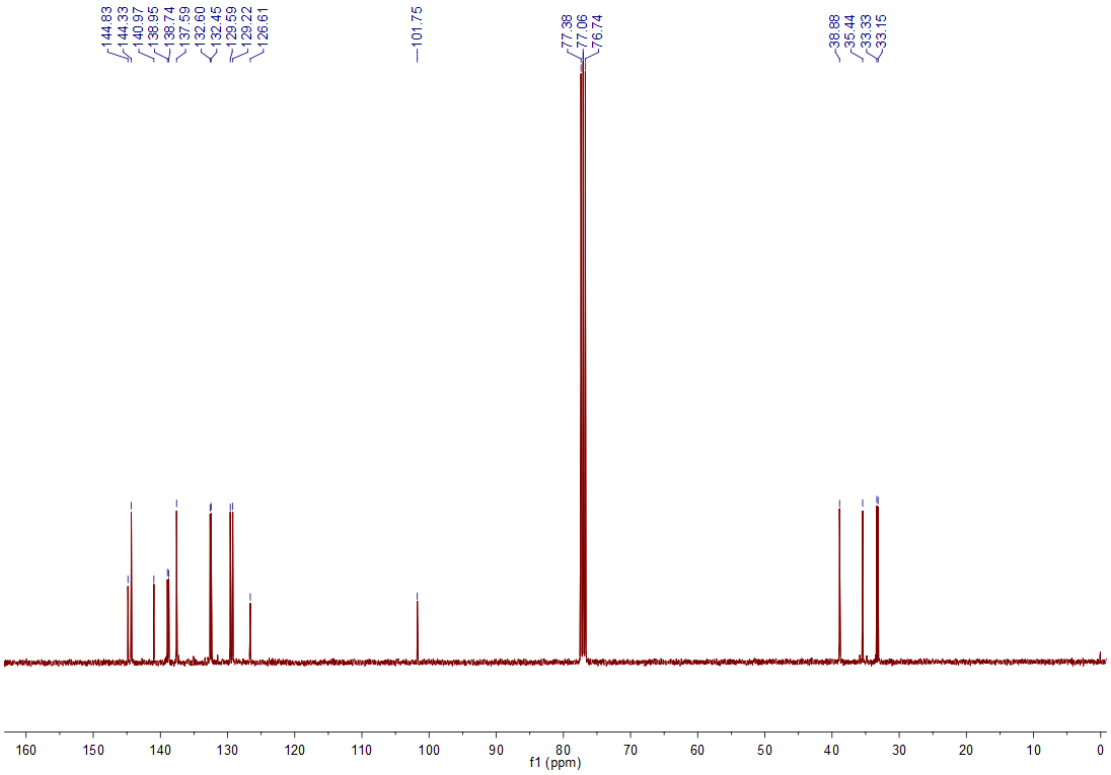

Fig. S6. ^{13}C NMR spectrum of *rac*-**I-PCP-Br**.

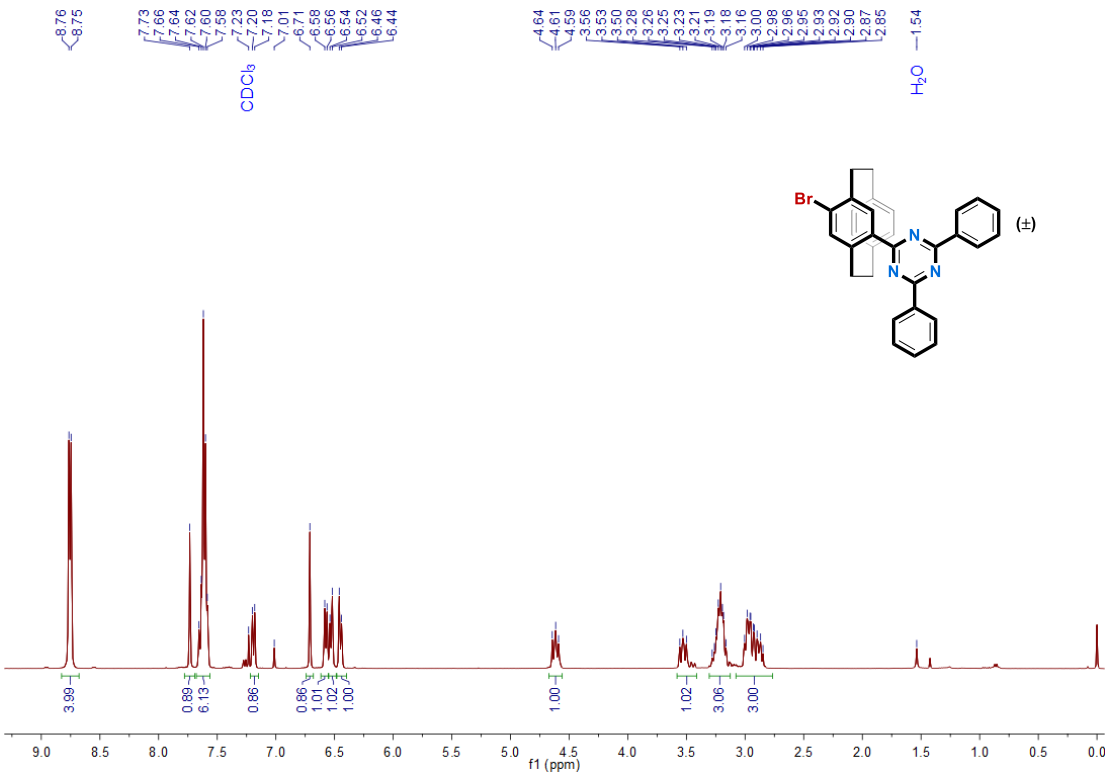

Fig. S7. ^{1}H NMR spectrum of *rac*-**Br-PT**.

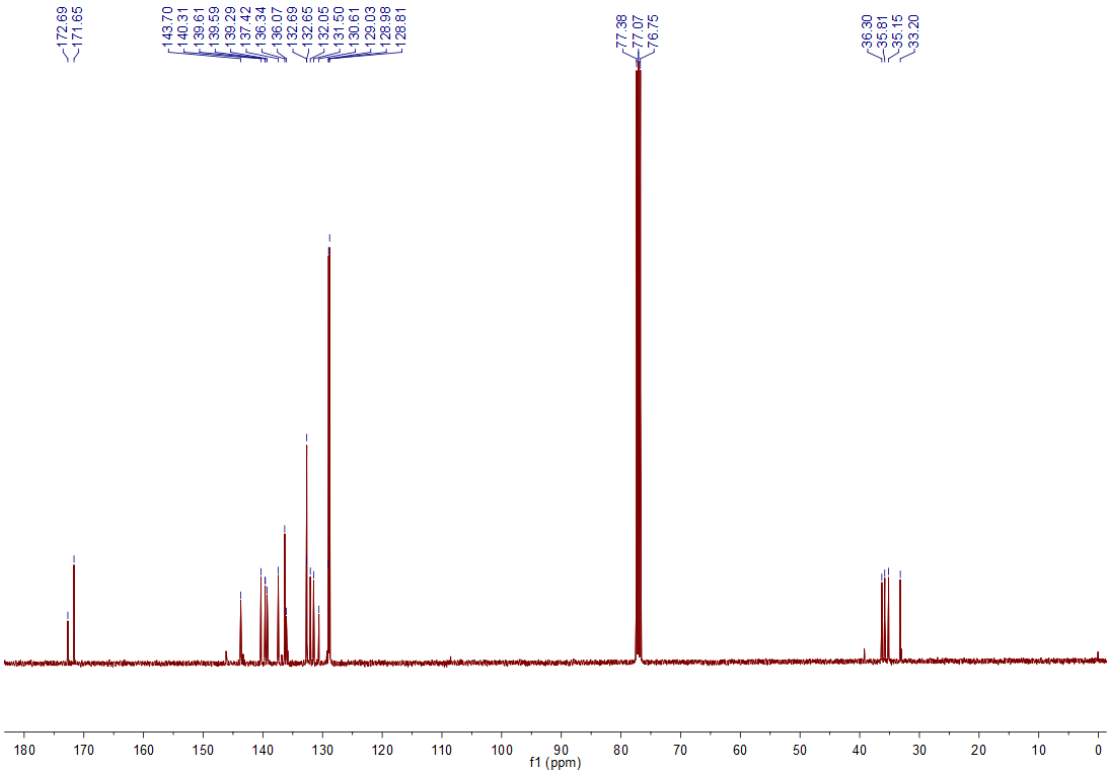

Fig. S8. ^{13}C NMR spectrum of *rac*-**Br-PT**.

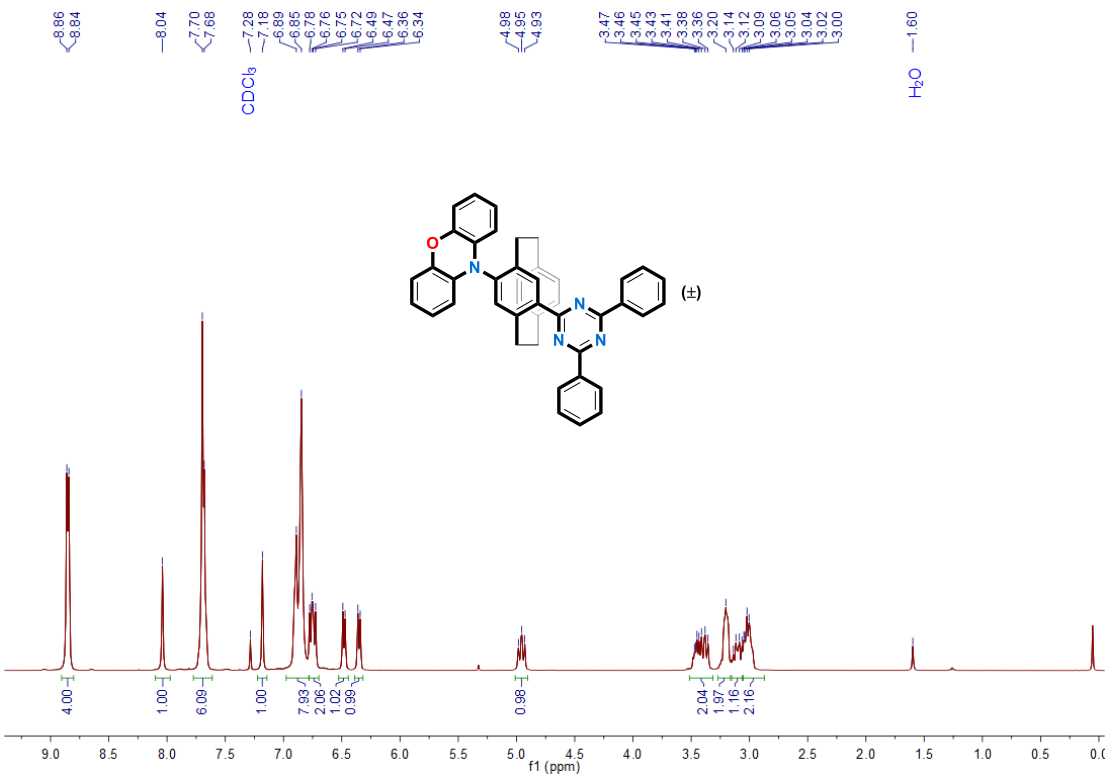

Fig. S9. ^{1}H NMR spectrum of *rac*-**PXZ-PT**.

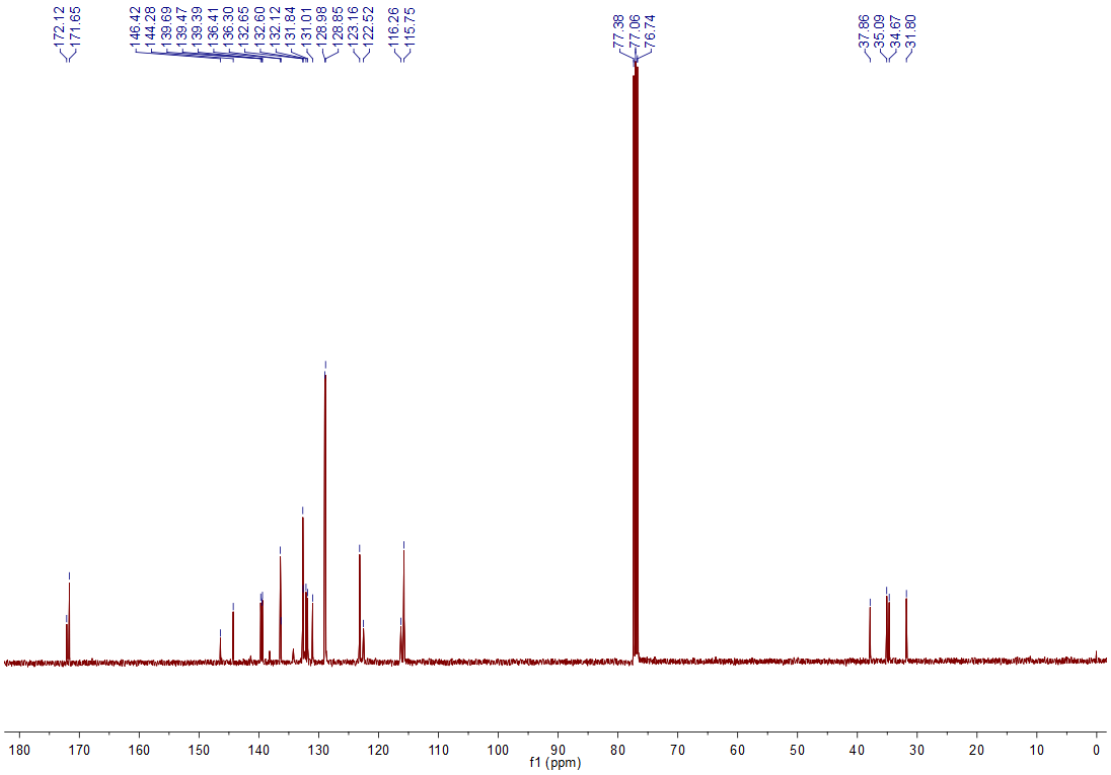

Fig. S10. ^{13}C NMR spectrum of *rac*-**PXZ-PT**.

2.3 High-resolution mass analyses

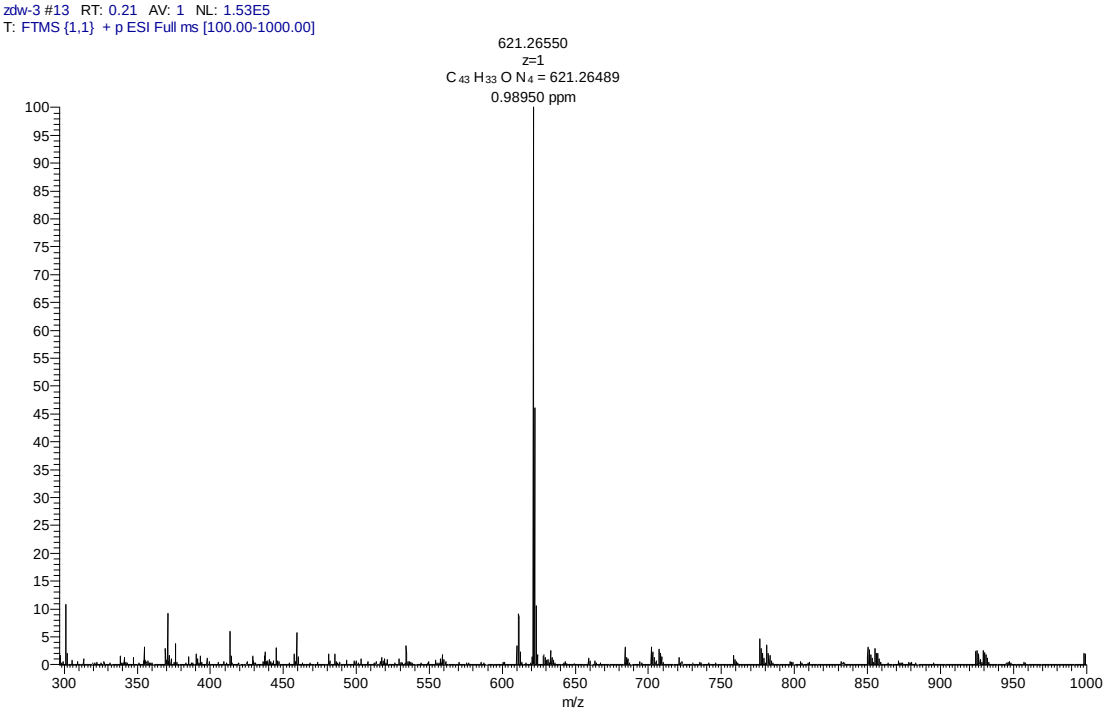

Fig. S11. High-resolution mass analyses of *rac*-**PXZ-PT**.

2.4 Single crystal structures

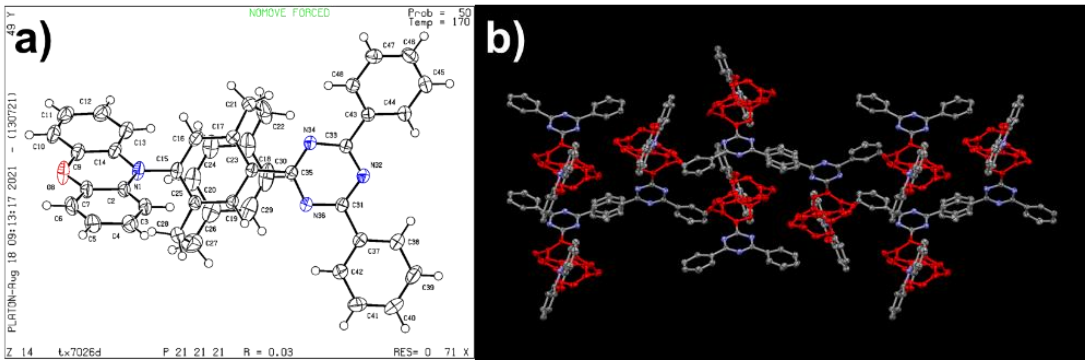

Fig. S12. a) Ellipsoid plot diagram of crystal structure of *R*-**PXZ-PT**. b) The packing of *R*-**PXZ-PT**. The molecules marked in red were of *R* configuration.

Table S1 Crystal data and structure refinement for *R*-**PXZ-PT**.

Parameter	*R*-**PXZ-PT**
CCDC Number	2103898
Identification code	TX7026D

Empirical formula	$C_{43}H_{32}N_4O$
Formula weight	620.72
Temperature/K	170.01(18)
Crystal system	orthorhombic
Space group	$P2_12_12_1$
a/Å	8.29020(10)
b/Å	12.93280(10)
c/Å	29.8623(2)
α/°	90
β/°	90
γ/°	90
Volume/Å^3	3201.70(5)
Z	4
ρ_{calc}g/cm^3	1.288
μ/mm^{-1}	0.610
F(000)	1304.0
Crystal size/mm^3	0.4 × 0.24 × 0.2
Radiation	Cu Kα (λ = 1.54184)
2Θ range for data collection/°	5.92 to 150.552
Index ranges	-10 ≤ h ≤ 10, -16 ≤ k ≤ 15, -37 ≤ l ≤ 37
Reflections collected	43970
Independent reflections	6470[R_{int} = 0.0330, R_{sigma} = 0.0168]
Data/restraints/parameters	6470/0/433
Goodness-of-fit on F^2	1.031
Final R indexes [I>=2σ (I)]	R_1 = 0.0316, wR_2 = 0.0810
Final R indexes [all data]	R_1 = 0.0323, wR_2 = 0.0817
Largest diff. peak/hole / e Å^{-3}	0.13/-0.21
Flack parameter	-0.06(8)

3. Photophysical properties

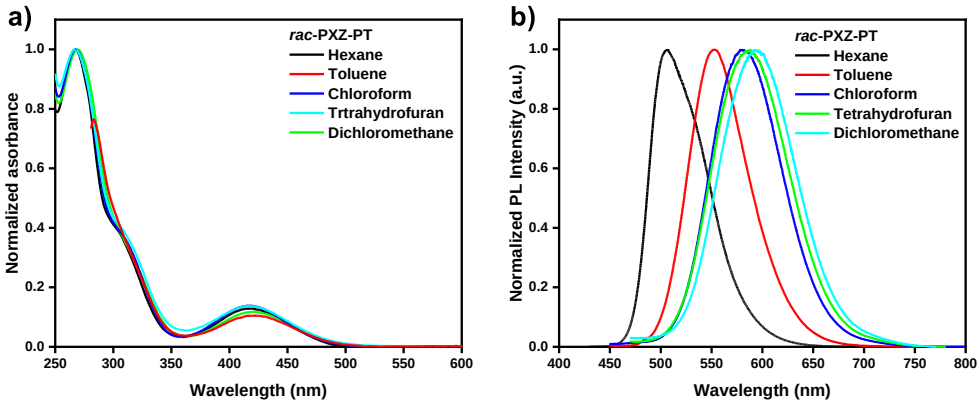

Fig. S13. a) UV-vis absorption spectra of *rac*-**PXZ-PT** in various solution (10^{-5} mol/L); π-π* transition was not observed in toluene due to the toluene cut-off. The high intense absorption peak at 268 nm was ascribed π-π* transition. The lower-energy absorption peak at 421 nm was assigned to the intramolecular charge-transfer (ICT) from **PXZ** donor to **PT** acceptor. b) Solvatochromic effect of *rac*-**PXZ-PT** measured in various solvents (10^{-5} mol/L).

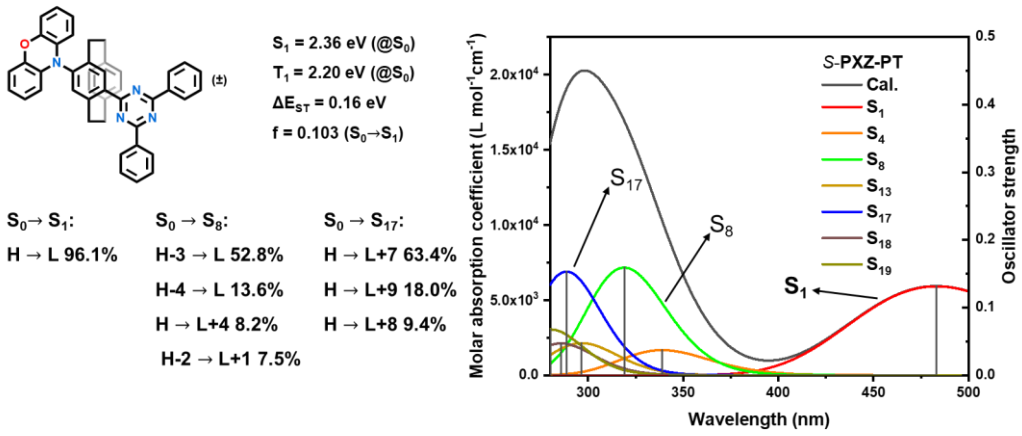

Fig. S14. Theoretical absorption spectra of *S*-**PXZ-PT** simulated with TD-DFT at the b3lyp/6-31g(d) level under the SMD toluene solvent model (right) and corresponding major molecular orbitals in excited states (left). It tended to underestimate the excitation energy to afford slightly red-shifted theoretical spectra.

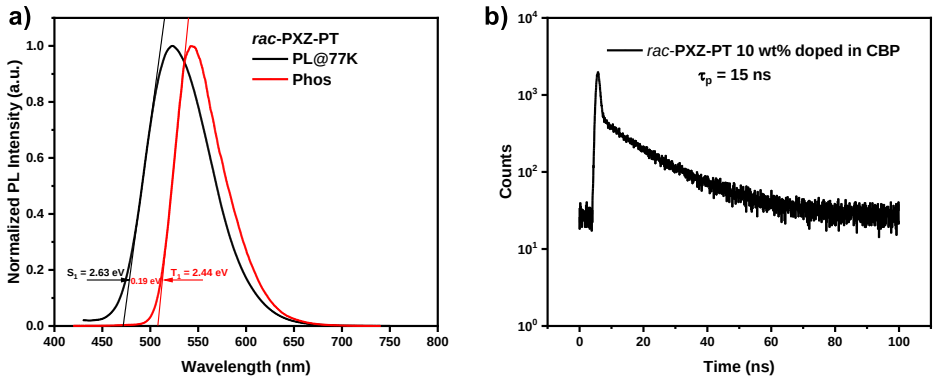

Fig. S15. a) Normalized fluorescence and phosphorescence spectra in 2-methyltetrahydrofuran at 77K for *rac*-**PXZ-PT**. b) Transient PL decay curves for the doped film of 10 wt% *rac*-**PXZ-PT** in a CBP host matrix at 298K.

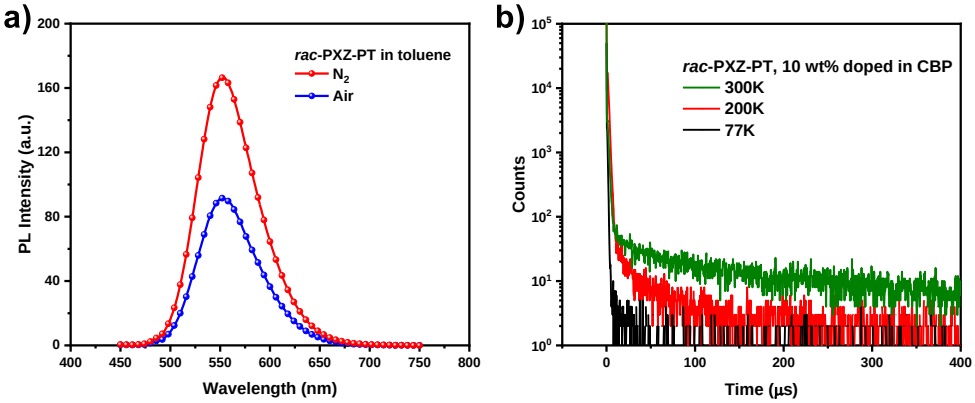

Fig. S16. a) PL spectra for *rac*-**PXZ-PT** in dilute toluene before and after nitrogen purging. b) Temperature dependence of time-resolved PL lifetime of *rac*-**PXZ-PT** in 10 wt% CBP film (λ_{exc} = 377.3 nm).

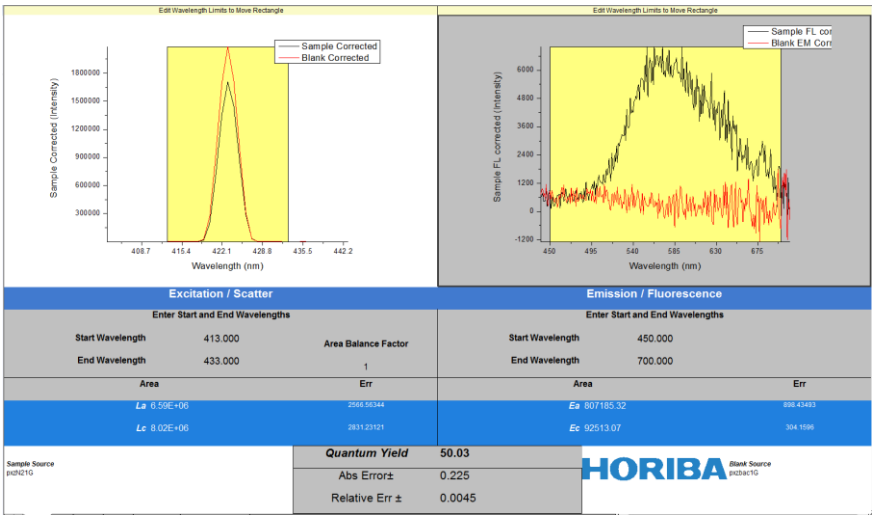

Fig. S17. PLQY of *rac*-**PXZ-PT** in dilute toluene (the absorbance was 0.06, filed with N_2).

Scheme S7. The rate constants of intersystem crossing (k_{ISC}) and reverse intersystem crossing (k_{RISC}) of the emitter based on the following equations[S4]:

$k_{\mathrm{p}} = \frac{1}{\tau_{\mathrm{p}}}$ k_{p}: Prompt fluorescence decay rate.

$k_{\mathrm{d}} = \frac{1}{\tau_{\mathrm{d}}}$ k_{d}: Delayed fluorescence decay rate.

$\Phi_{\mathrm{PL}} = \frac{k_{\mathrm{p}}}{k_{\mathrm{p}}+k_{\mathrm{IC}}}$ k_{IC}: internal conversion rate.

$k_{\mathrm{r,s}} = k_{\mathrm{p}}\Phi_{\mathrm{p}} + k_{\mathrm{d}}\Phi_{\mathrm{d}} \approx k_{\mathrm{p}}\Phi_{\mathrm{p}}$ $k_{r,s}$: Radiative decay rate from a singlet excited state.

$k_{\mathrm{ISC}} \approx (1-\Phi_{\mathrm{p}})k_{\mathrm{p}}$ k_{ISC}: Intersystem crossing rate.

$k_{\mathrm{RISC}} \approx \frac{k_{\mathrm{p}}k_{\mathrm{d}}}{k_{\mathrm{ISC}}} \cdot \frac{\Phi_{\mathrm{d}}}{\Phi_{\mathrm{p}}}$ k_{RISC}: Reverse intersystem crossing rate.

Table S2 Summary of physical properties of *R*/*S*-**PXZ-PT**.

Compound	$\lambda_{abs}/\lambda_{em}$[a] [nm]	ΔE_{ST}[b] [ev]	τ_p[c] [ns]	τ_d[d] [μs]	*HOMO/LUMO*[e] [eV]	Φ_{PL}[g] [%]	$k_{r,s}$[h] [10^7 s^{-1}]	k_{RISC}[i] [10^4 s^{-1}]	g_{lum}[j] [10^{-3}]
PXZ-PT	421/565	0.19	15	75	-5.15/-2.76(-2.70)[f]	78	3.60	1.21	±1.9

[a]Measured in toluene, 1.0×10^{-5}M. [b]ΔE_{ST} measured in 2-MeTHF at 77K. [c]Lifetime of the prompt components as determined from transient decay spectrum. [d]Lifetime of the delayed components as determined from transient decay spectrum. [e]HOMO and LUMO levels are determined from the onset of the oxidation curves and reduction curves. [f]LUMO levels are calculated by using the HOMO levels and $E_{g,opt}$. [g]Φ_{PL} measured under vacuum in 10wt%-doped film in CBP host matrix. [h]calculated radiative decay rate from a singlet excited state. [i]calculated reverse intersystem crossing rate constant. [j]Measured in toluene, 1.0×10^{-5}M.

Table S3. The quantum yields, lifetimes, and transition rate constants of *R*/*S*-**PXZ-PT**.

Compound	$\Phi_{PL}/\Phi_p/\Phi_d$	τ_p/τ_d	k_p [10^7 s^{-1}]	k_d [10^4 s^{-1}]	$k_{r,s}$ [10^7 s^{-1}]	K_{IC} [10^7 s^{-1}]	k_{ISC} [10^7 s^{-1}]	k_{RISC} [10^4 s^{-1}]
R/*S*-**PXZ-PT**	0.67/0.47/0.21	15ns/75μs	6.67	1.25	3.60	1.88	3.07	1.21

4. Electrochemical and TGA measurements

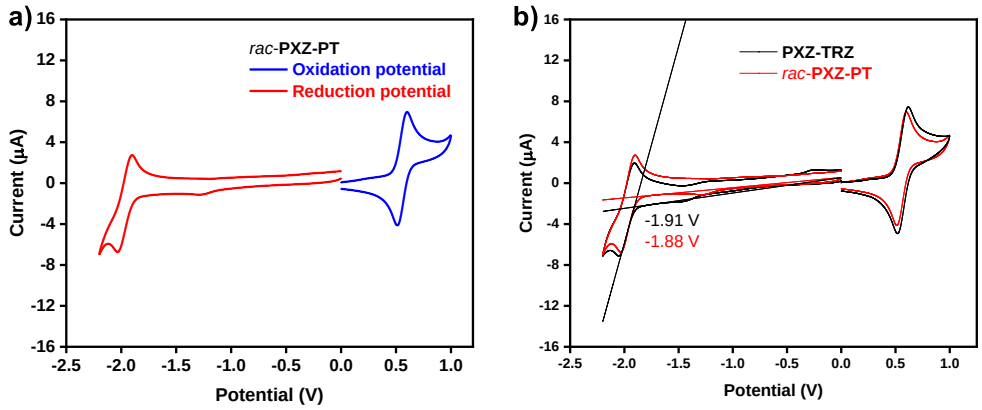

Fig. S18. a) Cyclic voltammetry characteristic curve of *rac*-**PXZ-PT**. b) Comparison of cyclic voltammetry characteristic curves of **PXZ -TRZ** and *rac*-**PXZ-PT**.

Table S4. Electrochemical properties of *rac*-**PXZ-PT**.

Compound	E_{ox}	E_{red}	$E_{HOMO,\,CV}$	$E_{LUMO,\,CV}$	$E_{g,\,elec}{}^{a}$	$E_{g,\,opt}{}^{b}$	$E_{LUMO}{}^{c}$
rac-**PXZ-PT**	0.49 V	-1.88 V	-5.15 eV	-2.76 eV	2.39 eV	2.45 eV	-2.70 eV

[a]Calculated by $E_{HOMO,\,CV}$ - $E_{LUMO,\,CV}$. [b]Determined from the onset of its UV–vis absorption spectrum. [c]E_{LUMO} = $E_{HOMO,\,CV}$ + $E_{g,\,opt}$.

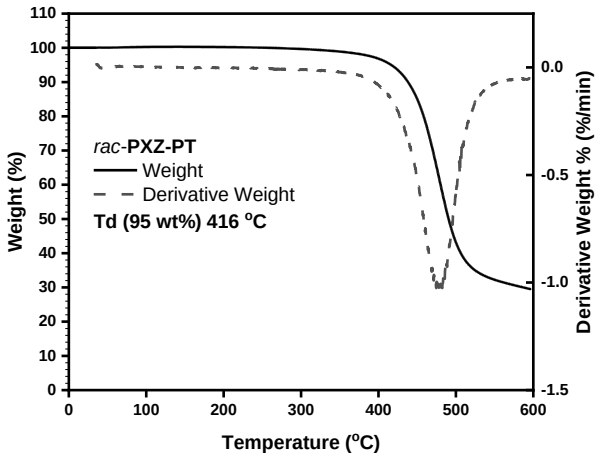

Fig. S19. TGA curve of *rac*-**PXZ-PT**.

5. Chiroptical data

Chiral HPLC Analysis

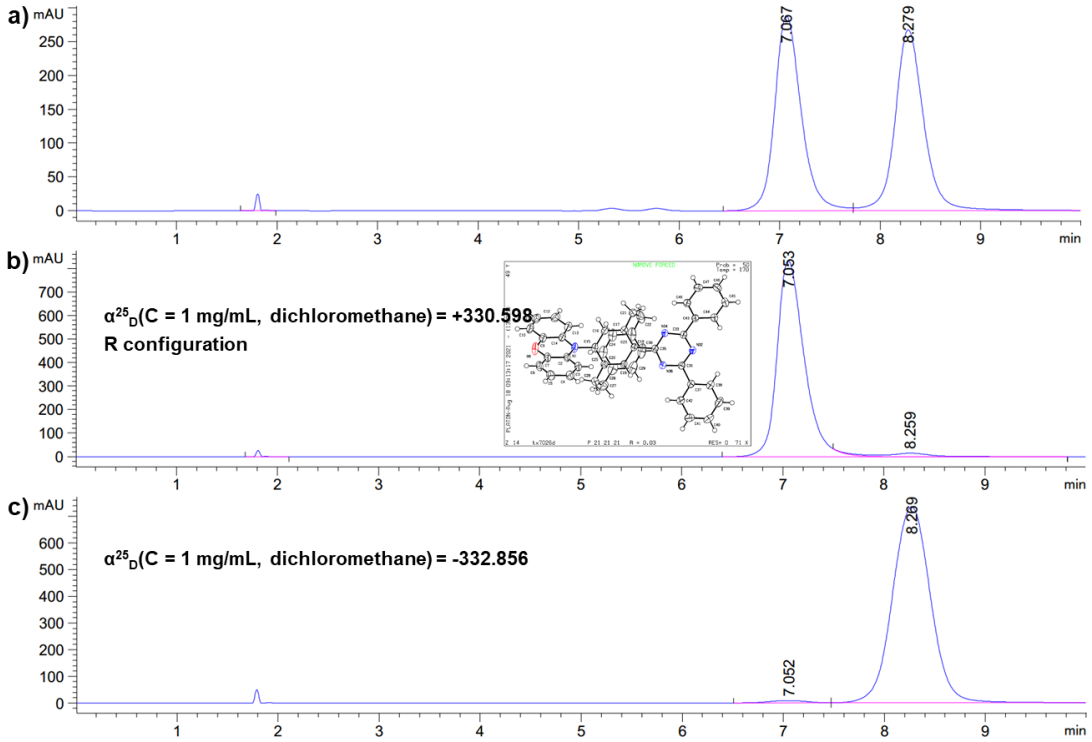

Fig. S20. Chiral HPLC analysis of a) *rac*-**PXZ-PT**, b) *R*-**PXZ-PT**, c) *S*-**PXZ-PT**. (IF, *n*-hexane/dichloromethane 85:15, 2 mL/min). The front fraction time component is identified as *R* configuration through enantiomer single crystal.

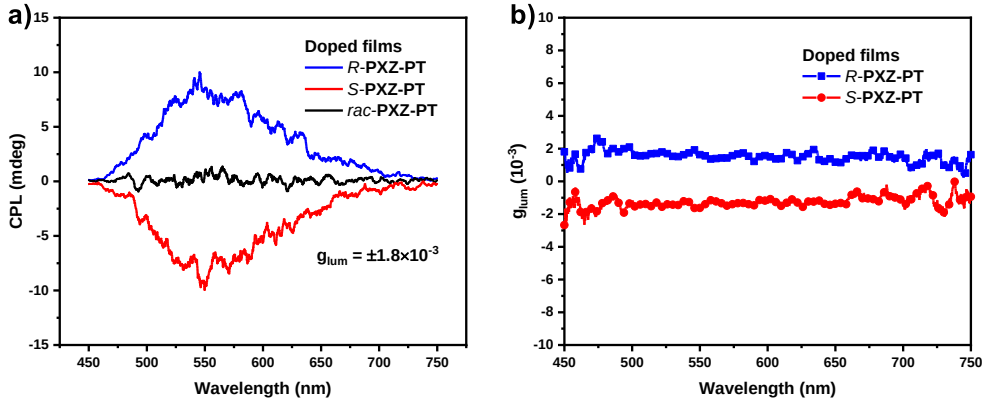

Fig. S21. a) CPL spectra of *R*/*S*/*rac*-**PXZ-PT** doped in CBP matrix with the doping ratio of 10 wt%. (λ_{exc} = 337 nm); b) g_{lum} -wavelength characteristics of *R*/*S*-**PXZ-PT**.

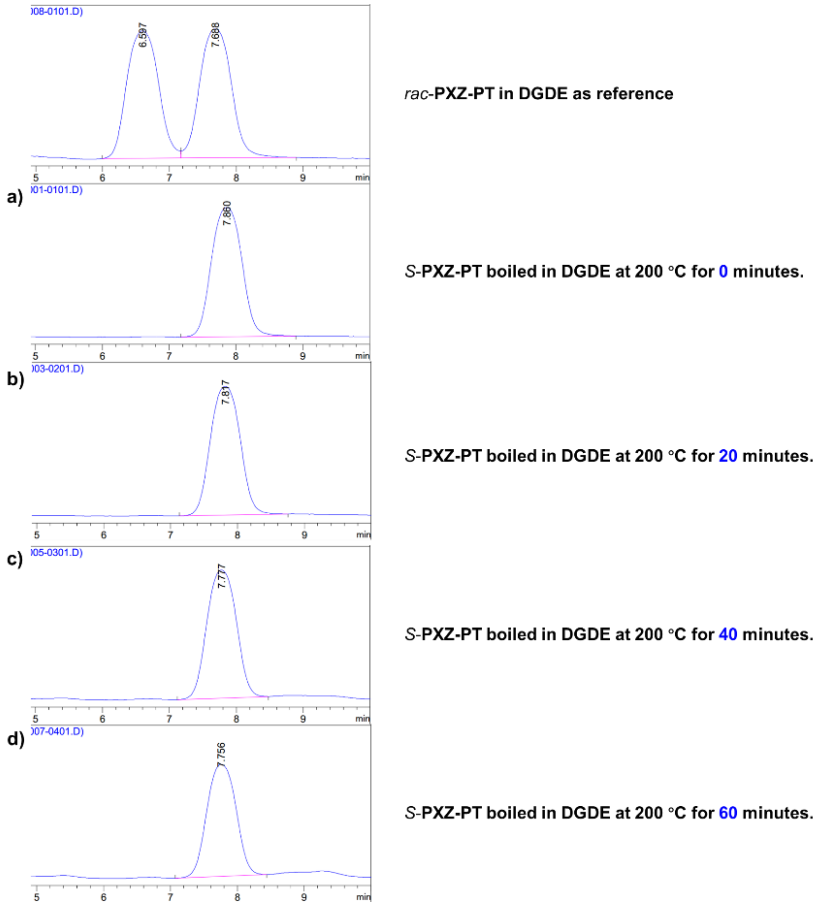

Fig. S22. Chiral HPLC analysis result of *S*-**PXZ-PT** after boiling in DGDE at 200°C for a) 0 minutes, b) 20 minutes, c) 40 minutes, d) 60 minutes (IF, n-hexane/dichloromethane 85:15, 2 mL/min, DGDE represent diethylene glycol dibutyl ether).

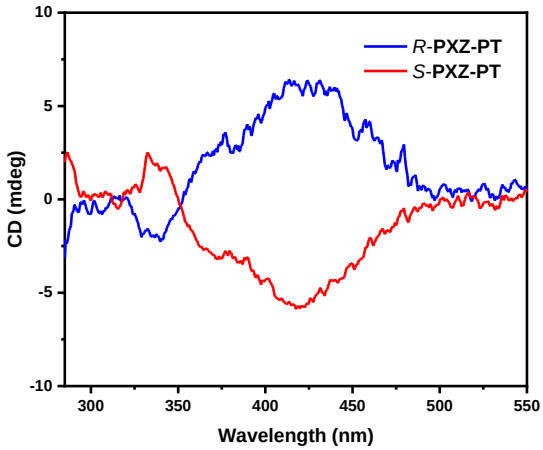

Fig. S23. The *R*/*S*-**PXZ-PT** taken out of the crucible after finishing fabricating the devices.

6. Device fabrication and characterization

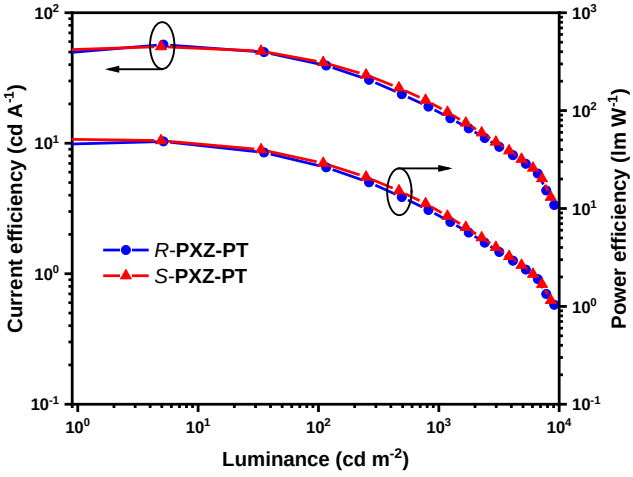

Fig. S24. Current efficiency-luminance -power efficiency characteristics of CP-OLEDs fabricated with *R*/*S*-**PXZ-PT**.

7. Representative planar chiral TADF molecules

Table S5. Representative planar chiral TADF molecular structures and their corresponding CP-OLED performance.

Planar chiral TADF emitters	EQE_{max}	g_{lum}	g_{EL}	*Ref.*
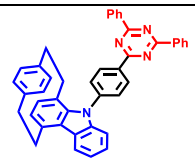 Zysman-Colman *et al. Chem. Sci.* **2019.**	17.0%	+1.2/-1.3×10^{-3}	-	S5
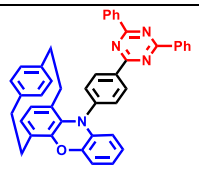 Zheng *et al. ACS Appl. Interfaces* **2021.**	8.7%	+3.3/-2.4×10^{-3}	+4.3/-4.6×10^{-3}	S6
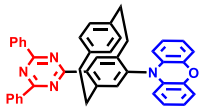	20.1%	±1.9×10^{-3}	+1.8/-1.3×10^{-3}	This work
TADF emitter (PXZ-TRZ)				
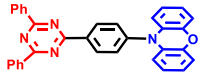 Adachi *et al. Chem. Mater.*, **2021.**	13.3%	-	-	S7

8. References

[S1] Gaussian 09, Revision D.01, M. J. Frisch, G. W. Trucks, H. B. Schlegel, G. E. Scuseria, M. A. Robb, J. R. Cheeseman, G. Scalmani, V. Barone, B. Mennucci, G. A. Petersson, H. Nakatsuji, M. Caricato, X. Li, H. P. Hratchian, A. F. Izmaylov, J. Bloino, G. Zheng, J. L. Sonnenberg, M. Hada, M. Ehara, K. Toyota, R. Fukuda, J. Hasegawa, M. Ishida, T. Nakajima, Y. Honda, O. Kitao, H. Nakai, T. Vreven, J. A. Montgomery, Jr., J. E. Peralta, F. Ogliaro, M. Bearpark, J. J. Heyd, E. Brothers, K. N. Kudin, V. N. Staroverov, T. Keith, R. Kobayashi, J. Normand, K. Raghavachari, A. Rendell, J. C. Burant, S. S. Iyengar, J. Tomasi, M. Cossi, N. Rega, J. M. Millam, M. Klene, J.25 E. Knox, J. B. Cross, V. Bakken, C. Adamo, J. Jaramillo, R. Gomperts, R. E. Stratmann, O. Yazyev, A. J. Austin, R. Cammi, C. Pomelli, J. W. Ochterski, R. L. Martin, K. Morokuma, V. G. Zakrzewski, G. A. Voth, P. Salvador, J. J. Dannenberg, S. Dapprich, A. D. Daniels, O. Farkas, J. B. Foresman, J. V. Ortiz, J. Cioslowski, and D. J. Fox, Gaussian, Inc., Wallingford CT, 2013.

[S2] P. Schaal, H. Baars, G. Raabe, I. Atodiresei, C. Bolm, *Adv. Synth. Catal.*, 2013, **355**, 2506.

[S3] F. He, Y. Ma, L. Zhao, W. Duan, J. Chen, C. Song, *Org. Lett.*, 2012, **14**, 21.

[S4] K. Goushi, K. Yoshida, K. Sato, C. Adachi, *Nature Photon.*, 2012, **6**, 253.

[S5] N. Sharma, E. Spuling, C. M. Mattern, W. Li, O. Fuhr, Y. Tsuchiya, C. Adachi, S. Bräse, I. D. W. Samuel, E. Zysman-Colman, *Chem. Sci.*, 2019, **10**, 6689.

[S6] C. Liao, Y. Zhang, S.-H. Ye, W.-H. Zheng, *ACS Appl. Mater. Interfaces*, 2021, **13**, 25186.

[S7] H. Tanaka, K. Shizu, H. Nakanotani, C. Adachi, *Chem. Mater.*, 2013, **25**, 3766.

9. Computational geometry data

Geometrically optimized Cartesian coordinates in Å

(*S*)-**PXZ-PT** molecule

C	-0.17213300	1.56020100	-2.71791600
C	0.62043700	0.42034300	-2.86942300
C	0.04461100	-0.85785300	-2.90846200
C	-1.33951500	-0.91947900	-3.12203400
C	-2.13178900	0.21689300	-2.96467900
C	-1.56302800	1.44568700	-2.59762100
C	-2.38738700	2.45857500	-1.82885800
C	0.82116400	-2.06953600	-2.42717700
C	-2.25349700	-0.19678800	0.32898700
C	-1.52970700	-1.38081800	0.14938300
C	-0.14954300	-1.38828500	-0.11443800
C	0.55254600	-0.19689900	0.18065300
C	-0.18545100	0.99225000	0.30324600
C	-1.57496300	1.03893800	0.20720400
C	-2.23816900	2.32874000	-0.23297900
C	0.42403700	-2.52427600	-0.94795900
C	2.03174900	-0.11059200	0.24602400
N	-3.65833100	-0.19539600	0.60574000
N	2.72698400	-1.23313200	0.49282600
N	2.59788300	1.10008300	0.09724700
C	3.93405000	1.14407800	0.20520000
C	4.05915200	-1.09282800	0.58378800
C	4.86576200	-2.30631200	0.86056600
N	4.70723100	0.07336900	0.44488600
C	4.60140900	2.45917600	0.04507900
C	5.99288800	2.57141700	0.19303200

C	6.61840500	3.80661900	0.04335800
C	5.86427300	4.94366400	-0.25690400
C	4.47906500	4.83953400	-0.40608500
C	3.85004000	3.60626200	-0.25557100
C	6.26774700	-2.25140400	0.81489200
C	7.02461000	-3.39232000	1.06933000
C	6.39260500	-4.59941100	1.37829200
C	4.99790500	-4.66032000	1.43120700
C	4.23749400	-3.52244800	1.17258900
C	-4.08298400	0.33199700	1.85454900
C	-4.65691100	-0.78447300	-0.21133500
C	-4.41121300	-1.69558600	-1.24561400
C	-5.99769100	-0.41432600	0.01754600
C	-5.43418700	0.67564500	2.01964900
C	-3.22293400	0.50796100	2.94533300
C	-5.91150200	1.19929200	3.21351500
C	-5.03506300	1.40231600	4.28218100
C	-3.69414900	1.05109400	4.14325100
O	-6.33019200	0.52065800	0.97989400
C	-7.03896800	-0.93424700	-0.73886300
C	-6.77259700	-1.83226500	-1.77459700
C	-5.45550300	-2.20498900	-2.02389800
H	0.31146300	2.51768400	-2.53512600
H	1.70109300	0.51999500	-2.79784400
H	-1.81898700	-1.88563100	-3.27025700
H	-3.21357800	0.11494400	-2.98730500
H	-2.11582400	3.48573900	-2.09920600
H	-3.44545400	2.33203900	-2.08143100
H	0.67735500	-2.93904600	-3.08069800

H	1.89156200	-1.83769800	-2.43777100
H	-2.06656200	-2.32370100	0.11899300
H	0.37505000	1.91972500	0.34894000
H	-3.23024300	2.45029700	0.21003200
H	-1.62843100	3.16754000	0.11873700
H	-0.34191000	-3.30429600	-1.02274500
H	1.30907700	-2.97211300	-0.49346500
H	6.56790600	1.68285600	0.42716800
H	7.69591600	3.88324900	0.16118100
H	6.35390400	5.90687500	-0.37410300
H	3.88874100	5.72134100	-0.64006900
H	2.77597100	3.51371200	-0.36957900
H	6.74724200	-1.30917100	0.57520900
H	8.10919600	-3.34065900	1.02702200
H	6.98463300	-5.48860000	1.57855500
H	4.50243100	-5.59586700	1.67620200
H	3.15490500	-3.55699600	1.21899800
H	-3.39600000	-1.99064500	-1.46737700
H	-2.17969500	0.23134500	2.85063500
H	-6.96550800	1.44981300	3.28132000
H	-5.40415100	1.82463000	5.21194500
H	-3.00223900	1.18979200	4.96896300
H	-8.04858100	-0.60793300	-0.50977200
H	-7.58702500	-2.22947800	-2.37263800
H	-5.22349100	-2.90082500	-2.82520500